Journal Pre-proofs

Exploring morphological heterogeneity of circulating tumor cells: machine learning-based approach for cell identification and prognostic implications

Peng-Xiang Wang, Yu-Chen Zhong, Bin Duan, Jian-Wen Cheng, Yun-Fan Sun, Wen-Jing Zheng, Kai-Qian Zhou, Yang Xu, Hai-Xiang Peng, Wei-Xiang Jin, Hai-Min Li, Xiao-Juan Sun, Wei Guo, Jian Zhou, Qi Liu, Jia Fan, Xin-Rong Yang

PII: S2095-9273(25)00433-5
DOI: https://doi.org/10.1016/j.scib.2025.04.048
Reference: SCIB 3347

To appear in: *Science Bulletin*

Received Date: 20 October 2024
Revised Date: 28 December 2024
Accepted Date: 31 March 2025

Please cite this article as: P-X. Wang, Y-C. Zhong, B. Duan, J-W. Cheng, Y-F. Sun, W-J. Zheng, K-Q. Zhou, Y. Xu, H-X. Peng, W-X. Jin, H-M. Li, X-J. Sun, W. Guo, J. Zhou, Q. Liu, J. Fan, X-R. Yang, Exploring morphological heterogeneity of circulating tumor cells: machine learning-based approach for cell identification and prognostic implications, *Science Bulletin* (2025), doi: https://doi.org/10.1016/j.scib.2025.04.048

Exploring morphological heterogeneity of circulating tumor cells: machine learning-based approach for cell identification and prognostic implications

Peng-Xiang Wang[1†], Yu-Chen Zhong[1†], Bin Duan[2,3†], Jian-Wen Cheng[1†], Yun-Fan Sun[1], Wen-Jing Zheng[1], Kai-Qian Zhou[1], Yang Xu[1], Hai-Xiang Peng[4], Wei-Xiang Jin[4], Hai-Min Li[4], Xiao-Juan Sun[4], Wei Guo[5], Jian Zhou[1], Qi Liu[2*], Jia Fan[1*], Xin-Rong Yang[1*]

1. Department of Liver Surgery & Transplantation, Liver Cancer Institute, Zhongshan Hospital, Fudan University; Key Laboratory of Carcinogenesis and Cancer Invasion, Ministry of Education, Shanghai 200032, China

2. Translational Medical Center for Stem Cell Therapy and Institute for Regenerative Medicine, Shanghai East Hospital, Bioinformatics Department, School of Life Sciences and Technology, Tongji University, Shanghai 200092, China

3. Key Laboratory of Systems Biomedicine, Ministry of Education, Shanghai Center for Systems Biomedicine, Shanghai Jiao Tong University, Shanghai 200240, China

4. Dunwill Med-Tech, Shanghai 200032, China

5. Department of Laboratory Medicine, Zhongshan Hospital, Fudan University, Shanghai 200032, China.

† These authors contributed equally to this work.

* Corresponding authors.

Email addresses:

qiliu@tongji.edu.cn (Q. Liu),

fan.jia@zs-hospital.sh.cn (J. Fan),

yang.xinrong@zs-hospital.sh.cn (X.-R. Yang).

Received 20 Octorber 2024

Received in revised form 28 December 2024

Accepted 31 March 2025

Graphical abstract

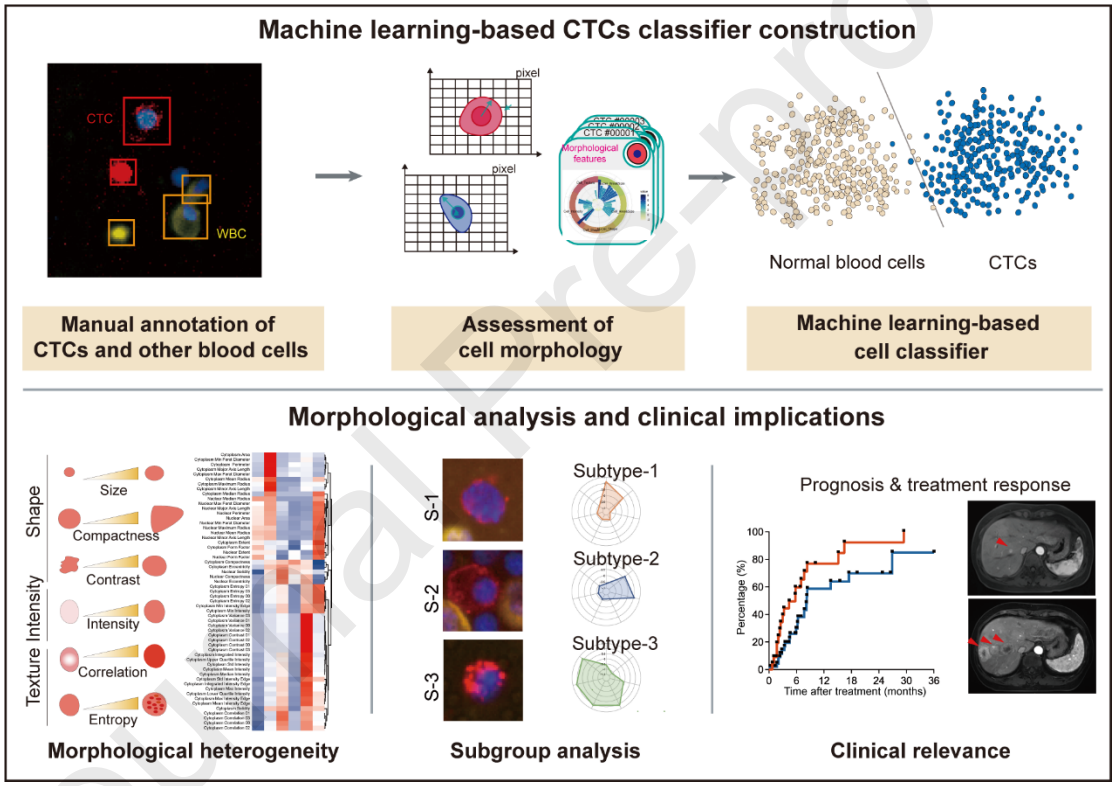

Main

Circulating tumor cells (CTCs), arising from the spread of primary or metastatic tumors, are crucial in understanding tumor metastasis. Unlike traditional serum biomarkers, CTCs, being actual tumor cells, offer more direct insight into the specific tumor's biology [1]. In the past decade, CTCs proved instrumental in the diagnosis of cancer, as well as for prognostic prediction, and monitoring the response to treatment [2]. Molecular profiling of CTCs offers a minimally-invasive window into the tumor's genetic and transcriptomic profiles, guiding precision or individualized oncology [3]. Phenotypic and functional analysis of CTCs not only enhances the detection of the cells, but also provides essential insights into tumor behavior that transcend simple enumeration [4]. However, the time- and labor-intensive visual examination of isolated fluorescence-labeled CTCs generally requires screening hundreds to thousands of cells in images and is prone to inaccuracies due to its reliance on human interpretation. Moreover, this process typically fails to fully capture the morphological diversity of CTCs, thus neglecting the full wealth of biological insights they might offer. Therefore, in-depth analysis of CTCs is of great interest for developing more effective treatment strategies.

In recent years, there have been significant developments in digitizing the analysis of medical images [5]. Algorithms can reveal and document numerous morphological features, which offers an opportunity for in-depth analysis of CTCs. In this study, we first trained a machine learning (ML)-based CTC identification model using 9692 CTC images from 1703 patients, achieving high accuracy in distinguishing CTCs from other circulating cells (Fig. 1a, Table S1 online) [6]. The morphological heterogeneity of these CTCs across cancers including hepatocellular carcinoma (HCC), gastric cancer (GC), cholangiocarcinoma (CCA), colorectal cancer (CRC), lung cancer (LC), and breast cancer (BRCA) were further explored. The study was approved by the Research Ethics Board of Zhongshan Hospital, Fudan University (B2021-288), with written informed consent obtained from every patient.

After being scanned using a PerkinElmer Operetta CLS (PerkinElmer, USA) and segmented by CellProfiler (Fig. 1b), these CTCs were characterized by multiple morphological parameters (57 major morphological features categorized into three groups: cell shape, fluorescence intensity, and cell texture, Fig. 1c, Table S2 online). We observed significant differences in cellular morphological features between CTCs and white blood cells (WBCs); CTCs demonstrated a larger cytoplasmic area, a slightly smaller nuclear area, and higher expression levels of EpCAM/pan-CK compared to WBCs (Fig. S1a–d online). Contrary to the commonly held belief that tumor cells are generally larger than white blood cells [7, 8], our results revealed significant heterogeneity in cell size among CTCs from different cancer types and underscored the potential overlap between WBCs and CTCs (Fig. 1d). Specifically, CTCs from CRC tend to have smaller diameters compared to WBCs ($P < 0.05$, *t*-test), whereas CTCs from CCA and BRCA exhibited a shift toward larger diameters. Notably, CTCs derived from HCC display a bimodal distribution, suggesting the presence of distinct morphological subpopulations. This variability highlights the morphological diversity of CTCs across cancer types and also suggests that a CTC isolation strategy based

solely on cell size may result in lower CTC purity or the exclusion of some CTCs subtypes.

Due to the complexity and subtle nature of morphological differences, traditional manual identification methods are both time-consuming and prone to error. Artificial intelligence algorithms, particularly those incorporating a range of markers for identification, offer a more efficient and accurate solution to these challenges [9]. Therefore, we applied ML-based algorithms to train on extracted cellular features, enabling us to develop our classification model (Fig. 1e). We selected the Extreme Gradient Boosting algorithm (XGBoost) to address the significant numerical imbalance between isolated CTCs and WBCs. The model achieved high efficiency in distinguishing CTCs across different cancer types, with an area under the receiver operating characteristic curve (AUC-ROC) exceeding 0.99 and an area under the precision-recall curve (AUC-PR) reaching 0.869 (Fig. S1e online). Among the morphological parameters, fluorescence intensity and texture entropy represented the top crucial features contributing to the ML-based identification model (Fig. S1f online). The ROC-AUC values for each cancer type were close to 1, indicating that the classifier still demonstrated strong overall performance in distinguishing CTCs from WBCs. However, the PR-AUC values varied, and the PR-AUC for CRC (0.358) was relatively weaker. This discrepancy may be attributed to the limited number of CTC samples available for these cancer types or morphological similarity between CRC CTCs and WBCs, making classification more challenging (Fig. S1g online). The overall performance of CTC identification was further validated using a chronological validation set comprising 8672 CTC images from 1621 patients, achieving an AUC-ROC > 0.99 and an AUC-PR of 0.819 (Fig. 1f, Table S3 online). Together, our study established a CTC morphological database and an automatic method for CTC identification powered by ML. We believe this image recognition approach holds potential for the accurate and efficient CTC detection in clinical practice, while future studies with more balanced datasets are warranted.

We next performed a comprehensive morphological analysis among CTCs originating from different cancer types. Similar to primary tumor cells, we found that CTCs exhibited considerable heterogeneity in features such as cell size, shape regularity, and fluorescent characteristics. The total CTCs could be classified into six distinct clusters based on morphological profiles (Fig. 1g–h, Fig. S2a online), where cluster 1 dominated making up 34.2% (3317 cells) of the total CTCs and the other clusters ranged from 11.1% to 15.6%. To evaluate whether cancer type-specific cellular features of CTCs exist, we displayed and compared morphological features across different tumor types (Fig. 1i, Fig. S2b online). LC tended to have a larger nuclear size and higher cytoplasmic texture entropy, CCA showed a trend toward larger overall cell sizes, and BRCA displayed stronger cytoplasmic epithelial marker intensity (Fig. S2c online). We hypothesized that these morphological differences is related to the histological origins of primary tumors, offering clues about the possible origin of tumors (Cramer's V = 0.528, Fig. 1j). Spearman's correlation analysis further corroborated this notion, revealing a significant association of CTCs from LC with cluster 3, a CTC subtype characterized by compact

cellular profiles but enlarged nuclei (Fig. 1k, Table S4 online). Additionally, when evaluating the morphological diversity across cancers, CTCs from HCC patients demonstrated the highest Gini-Simpson index and the lowest evenness index, highlighting the significant morphological diversity within this cancer type (Fig. 1l). While this diversity may, to some extent, be influenced by the relatively high number of CTCs detected in HCC in this study. In summary, our analyses highlight the heterogeneity of CTC morphology and suggest a potential correlation between CTC characteristics and the cancer type of origin. Such indications may provide clinicians with an accessible tool for tumor screening, guiding more targeted examinations and diagnosis.

We then focused our investigation on CTCs from HCC patients to explore the potential clinical implications of their pronounced morphological heterogeneity (Table S5 online). We identified three morphologically distinct subtypes of CTCs from HCC patients (Fig. 2a, Fig. S3a–b online). Among the subtypes, S-1 and S-2 CTCs had larger cell sizes than S-3. S-3 CTCs, despite being smaller, showed higher epithelial marker fluorescence intensity and more complex texture (Fig. 2b, Fig. S3c online). We found that the S-3 CTC subtype was strongly associated with tumor recurrence, with patients who experienced recurrence showing a significantly higher S-3 CTC load compared to those without recurrence (0.54 vs. 0.25, $P < 0.05$, Fig. 2c, Mann-Whitney test). Additionally, patients with a higher load of S-3 CTC had a greater likelihood of suffering early HCC recurrence within 24 months (57.2% vs. 32.1%, $P < 0.001$, Fig. S3d online, Chi-square test). Notably, patients exclusively harboring the S-3 CTC subtype exhibited a significantly higher rate of early tumor recurrence compared to those with S-2 CTCs (S-2 vs. S-3: $P = 0.012$, Fig. 2d). Additionally, there was a trend toward poorer prognosis in patients with S-3 CTCs compared to those with S-1 CTCs (S-1 vs. S-3: $P = 0.060$, Fig. 2d, Kaplan-Meier analysis). A subsequent survival analysis revealed that patients with S-3 CTCs exhibited the poorest clinical outcomes with regard to tumor recurrence ($P < 0.001$, Fig. 2e, Kaplan-Meier analysis), outperforming indicators using S-1/S-2 CTCs (Fig. S3e–f online). The presence of S-3 CTCs was significantly associated with larger tumor size ($P = 0.013$) and was marginally associated with poorer tumor differentiation ($P = 0.067$, Table S6 online, Chi-square test). Univariate and multivariate Cox regression analyses demonstrated that the presence of S-3 CTCs was an independent prognostic factor after adjusting for other established prognostic factors (hazard ratio [HR] = 2.04, 95% confidence interval [95% CI] = 1.45 – 2.87, $P < 0.001$, Table S7 online, Wald test). Based on these findings, we suggested that S-3 CTCs may represent a critical subset of CTCs involved in tumor seeding and metastasis (Fig. S3g online). Consistent with our initial findings, we observed that patients in an independent validation cohort with detectable S-3 CTCs prior to surgery had a significantly shorter time to recurrence (TTR) and a higher likelihood of recurrence (Fig. 2f, Table S8 online), whereas the presence of S-1/S-2 CTCs did not significantly impact prognostic outcomes ($P > 0.05$, Fig. S3h–I online). Moreover, S-3 CTCs remained an independent prognostic factor in the multivariate Cox analysis in this validation cohort (HR = 3.86, 95% CI = 1.21–12.34, $P = 0.023$, Table S9 online, Wald test). Thus, we found that the morphological subtypes of CTCs could

provide additional prognostic information for HCC patients, and specifically, S-3 CTCs might represent a subset of tumor cells with elevated metastatic potential which are closely associated with disease progression.

Immunotherapy has revolutionized the treatment of cancer in recent years, leading to substantial improvements in clinical outcomes [10,11]. We herein investigated whether our morphological subtyping of CTCs could serve as an indicator of the immunotherapeutic response in HCC patients. We enrolled 70 HCC patients who were scheduled to receive anti-programmed cell death protein 1 antibody (anti-PD-1) antibody-based treatment, fifty-four (77.1%) of whom were classified into Chinese Liver Cancer (CNLC) stage III-IV (Table S5 online). We observed that patients harboring S3-CTCs exhibited a significantly lower disease control rate (DCR, 22.2% vs. 53.6%; $P = 0.005$) and the overall response rate (ORR, 0% vs. 21.5%; $P = 0.0163$; Fig. 2g, Chi-square test) compared to those without S-3 CTCs. And patients with detectable S-3 CTCs before PD-1 treatment had a significantly shorter progression-free internal (PFI) compared to those without S-3 CTCs (5.7 vs. 8.3 months, $P = 0.020$; Fig. 2h, Kaplan-Meier analysis). Moreover, CTC counts alone did not accurately differentiate patient responses to PD-1-based treatment ($P > 0.05$, Fig. S4a–b online, Kaplan-Meier analysis, Chi-square test). Representative magnetic resonance imaging (MRI) scans taken at baseline, at the time of the progressive disease (PD) and partial response (PR) was diagnosed for patients with and without S-3 CTCs are presented in Fig. 2i. The tumor tissues from patients positive for S-3 CTCs showed significantly lower infiltration of $CD8^+$ T cells ($P = 0.001$, Fig. S4c online, *t*-test) and $CD4^+$ T cells ($P = 0.002$, Fig. S4d online, *t*-test) compared to the others, suggesting that the microenvironment of the primary tumor is characterized by a "colder" immune status. These results suggest that S-3 CTCs could serve as a novel predictive biomarker for immunotherapy resistance, underscoring the need for more frequent monitoring and early therapeutic interventions in patients with S-3 CTCs. Due to the limited number of cases, it is currently challenging to explore the relationship between CTC-subtype and treatment efficacy in other cancer types, warranting further investigations.

We further sought to explore the molecular insights underlying the association between the CTC morphological subtypes and diverse prognoses. We found that both EpCAM ($P = 0.017$) and pan-CK ($P = 0.024$) were highly expressed in primary tumor cells from patients with detectable S-3 CTCs (Fig. S4e–f online, Mann-Whitney test), indicating S-3 CTCs are closely associated with tumor cells exhibiting an enhanced epithelial phenotype. We further performed an in-depth analysis utilizing our earlier published single-cell RNA-seq profiles of 113 CTCs isolated from HCC patients [12]. We defined the CTCs subset exhibiting greater transcriptomic levels of epithelial genes as highly epithelial S-3-like CTCs (Fig. 2j). We noticed that S-3-like CTCs were significantly featured with pathways related to Myc targets, oxidative phosphorylation, E2F targets, and the G2/M checkpoint ($P < 0.05$, $Log_2FC > 1$, Fig. 2k). Using multi-color fluorescence analysis, we confirmed the up-regulation of Myc in S-3 CTCs from HCC patients (73.7 vs. 23.8%, $P < 0.001$, $n = 61$, Fig. 2l, Chi-square test), suggesting that Myc activation may be essential in mediating metastatic potential for this CTC subtype.

We further evaluated the previously reported signature scores for stemness, proliferative capacity, chemoresistance, and T cell cytotoxicity resistance [13-16] (Table S10 online), and our analysis showed that epithelial CTCs exhibited an enhanced potential for these cellular phenotypes (all $P < 0.001$, Fig. 2m, *t*-test). And these phenotypes were positively correlated with their epithelial characteristics (Fig. S4g online, spearman correlation). Gene Set Enrichment Analysis (GSEA) analysis revealed that S-3-like CTCs were closely linked to glycolysis and Notch signaling pathways, while pathways involved in anti-tumor immunity were downregulated (Fig. S4h online). When examining the prognostic value of the top 20 upregulated genes in S-3-like CTCs using the TCGA_LIHC cohort (Table S11 online), we found that this curated signature was significantly associated with poor overall survival (OS) in HCC patients ($P = 0.024$**,** Fig. S4i online, Kaplan-Meier analysis). As the retention of epithelial features in tumor cells is essential for metastatic invasion and implantation [17], we hypothesize that the molecular alterations identified in S-3 CTCs may enhance their metastatic potential.

In conclusion, we conducted a comprehensive examination of the morphological features and heterogeneity of CTCs across a variety of cancer types, with a primary focus on HCC due to its predominance in our dataset. The ML-based model for CTC recognition developed here could significantly enhance the accuracy and feasibility of CTC analysis in the clinical setting. By characterizing distinct morphological subtypes of CTCs in HCC, our research offers valuable insights into tumor biology and aggressiveness, which could inform risk stratification and monitoring of therapeutic responses. This study underscores the clinical utility of leveraging CTC morphology as a novel non-invasive biomarker to advance oncological care. Future studies with larger and more diverse sample sizes are needed to further validate these findings across different tumor types.

References

[1] Keller L, Pantel K. Unravelling tumour heterogeneity by single-cell profiling of circulating tumour cells. Nat Rev Cancer 2019;19:553-567.

[2] Nikanjam M, Kato S, Kurzrock R. Liquid biopsy: current technology and clinical applications. J Hematol Oncol 2022;15:131.

[3] Liu X, Song J, Zhang H, et al. Immune checkpoint HLA-E:CD94-NKG2A mediates evasion of circulating tumor cells from NK cell surveillance. Cancer Cell 2023;41:272-287.

[4] Ring A, Nguyen-Sträuli BD, Wicki A, et al. Biology, vulnerabilities and clinical applications of circulating tumour cells. Nat Rev Cancer 2023;23: 95-111.

[5] Rajpurkar P, Lungren MP. The current and future state of AI interpretation of medical images. N Engl J Med 2023;388:1981-1990.

[6] Wang P-X, Sun Y-F, Jin W-X, et al. Circulating tumor cell detection and single-cell analysis using an integrated workflow based on ChimeraX® -i120 platform: a prospective study. Mol Oncol 2021;15:2345-2362.

[7] Vona G, Sabile A, Louha M, et al. Isolation by size of epithelial tumor cells: a new method for the immunomorphological and molecular characterization of circulatingtumor cells. Am J Pathol 2000;156:57-63.

[8] Warkiani ME, Khoo BL, Wu L, et al. Ultra-fast, label-free isolation of circulating tumor cells from blood using spiral microfluidics. Nat Protoc 2016;11:134-148.

[9] Wang Y-RJ, Wang P, Yan Z, et al. Advancing presurgical non-invasive molecular subgroup prediction in medulloblastoma using artificial intelligence and MRI signatures. Cancer Cell 2024;42: 1239-1257

[10] Sangro B, Sarobe P, Hervás-Stubbs S, et al. Advances in immunotherapy for hepatocellular carcinoma. Nat Rev Gastroenterol Hepatol 2021;18:525-543.

[11] Armstrong S, Prins P, He AR. Immunotherapy and immunotherapy biomarkers for hepatocellular carcinoma. Hepatoma Research 2021;2021:

[12] Sun Y-F, Wu L, Liu S-P, et al. Dissecting spatial heterogeneity and the immune-evasion mechanism of CTCs by single-cell RNA-seq in hepatocellular carcinoma. Nat Commun 2021;12:4091.

[13] Joung J, Kirchgatterer PC, Singh A, et al. CRISPR activation screen identifies BCL-2 proteins and B3GNT2 as drivers of cancer resistance to T cell-mediated cytotoxicity. Nat Commun 2022;13:1606.

[14] Mohan A, Raj Rajan R, Mohan G, et al. Markers and reporters to reveal the hierarchy in heterogeneous cancer stem cells. Front Cell Dev Biol 2021;9:668851.

[15] Guo J, Grow EJ, Yi C, et al. Chromatin and single-cell RNA-Seq profiling reveal dynamic signaling and metabolic transitions during human spermatogonial stem cell development. Cell Stem Cell 2017;21: 533-546.

[16] Zhou Y, Lu L, Jiang G, et al. Targeting CDK7 increases the stability of Snail to promote the dissemination of colorectal cancer. Cell Death Differ 2019;26:1442-1452.

[17] Padmanaban V, Krol I, Suhail Y, et al. E-cadherin is required for metastasis in multiple models of breast cancer. Nature 2019;573:439-444.

Conflict of interest

The authors declare that they have no conflict of interest.

Acknowledgments

This work was supported by the National Basic Science Center Project of China (82488101), the National Natural Science Foundation of China (82341027, 82072715, 62302336, 32341008, 62088101, and 82403435), National Ten-thousand Talent Program of China, Shanghai Municipal Science and Technology Major Project, the Shanghai Municipal Health Commission Collaborative Innovation Cluster Project (2019CXJQ02), the Shanghai Sailing program (21YF1407300), Shanghai Rising-Star Program (23YF1450200), the Project of Shanghai Municipal Health Commission (2022LJ005), the projects from the Shanghai Science and Technology Commission (21140900300 and 22S31901800), the Eastern Talent Program (leading project), Shanghai Pilot Program for Basic Research, Shanghai Science and Technology Innovation Action Plan-Key Specialization in Computational Biology, China Postdoctoral Science Foundation (2022M722418 and 2023T160485), the project from Shanghai Hospital Development Center (SHDC2023CRD025), the Projects from Science Foundation of Zhongshan Hospital, Fudan university (2021ZSCX28, 2020ZSLC31, and ZP2023-017).

Author contributions

Xin-Rong Yang, Jia Fan, and Qi Liu conceived and designed the research. Peng-Xiang Wang, Yu-Chen Zhong, Bin Duan, and Jian-Wen Cheng designed and conducted the assays. Jian Zhou and Wei Guo supervised the study. Yun-Fan Sun, Wen-Jing Zheng, Kai-Qian Zhou, and Yang Xu contributed to sample preparation and patient clinical information. Hai-Xiang Peng, Wei-Xiang Jin, Hai-Min Li, and Xiao-Juan Sun assisted in morphological and bioinformatics data analysis. Peng-Xiang Wang, Yu-Chen Zhong, and Bin Duan wrote the manuscript, and Xin-Rong Yang, Jia Fan, and Qi Liu revised the paper. All authors read and approved the manuscript.

Appendix A. Supplementary material

Supplementary data to this article can be found online.

Figure legend

Fig. 1. Accurate identification of CTCs and pan-cancer heterogeneity analysis using image recognition models. (a) The patient cohort and the analysis strategy of the study. (b) Preprocess workflow of CTC image identification. (c) Representative morphological features used in classifier construction. (d) Cell diameter range of CTCs and WBCs and their interquartile overlap. (e) Workflow of the construction of CTC identification system. (f) Receiver operating characteristic (ROC) curve and precision-recall (PR) curve analysis of the ML-based model for CTCs identification in validation cohort. (g) t-SNE plot and pie plot of 6 morphologic CTCs clusters discovered by consensus clustering, colored according to different clusters. (h) Representative images of 6 clusters of CTC. (i) t-SNE plots showed the distribution of CTC morphological clusters among different cancer types. (j) Composition of CTCs morphological clusters in different cancer types. (k) Correlation between different cancer types and CTC morphological clusters (Spearman correlation). (l) Morphological heterogeneity of 6 cancer types evaluated by Gini-Simpson index and Evenness index.

Fig. 2. S-3 CTCs from HCC represented a superior indicator for HCC progression. (a) t-SNE plot showing CTCs subtypes in the HCC cohort, colored by different subtypes. (b) left: Representative images of 3 CTC subtypes; right: Radar plot summarized morphological features of three subtypes of CTCs. (c) Counts of total CTC and each subtype in HCC patients with or without recurrence. (d) Kaplan-Meier analysis for time to recurrence (TTR) in HCC patients with single type of CTC detected. (e) Kaplan-Meier analysis for TTR in HCC patients with/without S-3 CTCs. (f) Kaplan-Meier analysis for TTR stratified by S-3 CTC positivity in validation cohort. (g) Differences in treatment response rate in HCC patients between S-3 CTC positive or S-3 CTC negative subgroups as evaluated by irRECIST criteria. (h) Kaplan-Meier analysis of the progression-free interval between S-3 CTC positive or S-3 CTC negative subgroups in immunotherapy cohort. (i) Representative MRI images for patients with or without S-3 CTC at the baseline and endpoint of PD-1 inhibitor treatment. (j) Strategy to define the highly epithelial S-3-like CTCs using transcriptomic data. (k) Enrichment analysis of up-regulated genes in S-3 like CTCs (Hallmark gene set). (l) Representative images of EpCAM/CK and Myc co-expression within S-3 CTC and other types of CTC (upper). Myc expression positivity in S-3 CTCs and other CTC subtypes (lower). (m) Gene set scoring for S-3 like CTCs and other CTCs.